Nonlinear reduced order modeling of complex wing models

X.Q. Wang, R. A. Perez, M. P. Mignolet, R. Capillon, Christian Soize

Nonlinear Reduced Order Modeling of Complex Wing Models

X.Q. Wang[1], Ricardo A. Perez[2], Marc P. Mignolet[3]
Arizona State University, Tempe, AZ 85287

Rémi Capillon[4], and Christian Soize[5]
Université Paris-Est, 77454 Marne-la-Vallee, France

The focus of this paper is on the identification of nonlinear reduced order models for the prediction of the geometrically nonlinear structural response of cantilevered structures, including the wing of the Predator. These models represent the extension to large displacements/rotations of the modal models used in the linear range. The identification of their coefficients is carried out here from a full finite element model of the structure in a commercial software, Nastran was used in the present effort. Issues encountered in the past in successfully carrying out this identification are revisited and clarified. The development of a nonlinear reduced order model for the Predator is then performed and validated demonstrating the capabilities of these reduced order models in connection with complex structural models.

I. Introduction

Many novel aircraft designs, such as the Predator and its successors, see Fig. 1, involve very high aspect ratio/very flexible wings that are likely to undergo large deformations when subjected to the aerodynamic forces expected during flight. The aeroelastic analysis of such vehicles is thus rendered difficult by the need to account for the nonlinear geometric effects induced by these large deformations. While such computations can be carried out with full finite element models, they are notably more difficult than their counterparts for the linear structure in which modal techniques can be used to dramatically simplify the structural model.

Figure 1. General Atomics Predator Unmanned Aircraft System (UAS) [1].

Nonlinear reduced order models, which are the equivalent to nonlinear geometric problems of the modal methods of linear structures, can be used instead of the full finite element model to provide a compact structural dynamic model that is straighforward to couple with the aerodynamic solver (linear or CFD). Of particular interest here are the nonlinear reduced order modeling methods which proceed *non-intrusively* from a full finite element model

[1] Associate Research Scientist, SEMTE, Faculties of Mechanical and Aerospace Engineering, Senior Member AIAA.
[2] Currently: Postdoctoral Fellow, Universal Technology, Inc., Member AIAA.
[3] Professor, SEMTE, Faculties of Mechanical and Aerospace Engineering, Associate Fellow AIAA.
[4] Research Assistant, Laboratoire Modélisation et Simulation Multi Echelle.
[5] Professor, Laboratoire Modélisation et Simulation Multi Echelle.

developed in a standard commercial code (Nastran will be used here), see [2] for a very recent review. These methods have progressed steadily over the last few years and have reached the point at which rather complex structural models can be very successfully modeled, such as the 96,000 degree-of-freedom 9-bay panel of Fig. 2, see [3] for modeling discussion.

The applications of these nonlinear reduced order modeling methods have primarily focused on panel-like structures and thus with all around supports (e.g. clamps) with the exception of [4] which focused on flat cantilevered structures, e.g. wing-like models. It was pointed out in that investigation that:

(i) there exists an inconsistency between the reduced order modeling approach which assumes that the material is linearly elastic in that the Green strain and the second Piola-Kirchhoff stress are linearly related (by the elasticity tensor) while typical commercial finite element codes based on updated Lagrangian formulations are akin to assuming the linear relationship between the Almansi strain and Cauchy stress tensors. These two assumptions are incompatible except in the linear, small deformation case.

(ii) there exists some purely numerical issues that are specific to cantilevered structure as the magnitude of their corresponding geometric nonlinearity is typically much smaller than for fully supported structures. An approach to avoid these numerical issues was demonstrated.

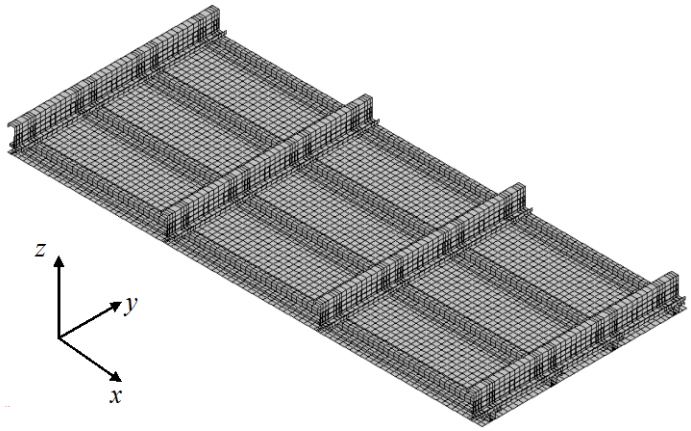

Figure 2. Finite element model of a 9-bay fuselage sidewall panel.

The focus of the present investigation is on extending the recent successes obtained with complex structures, see [3] and Fig. 2, to wing models. To this end, a revisit of the flat cantilevered beam will first be accomplished which will demonstrate the effects of the inconsistency discussed in (i) above and suggests a mitigation strategy. Next, a cantilevered curved beam will be considered to demonstrate the well foundedness of this strategy to curved structures. Finally, an extensive modeling of the wing of the Predator UAS of Fig. 1 will be carried which demonstrates the accuracy and effectiveness of the proposed nonlinear reduced order modeling method.

II. Nonlinear Reduced Order Modeling Overview

The reduced order modeling techniques considered here are based on the following modal-like representation of the nonlinear geometric response of the structure

$$\underline{u}(t) = \sum_{n=1}^{M} q_n(t)\, \underline{\psi}^{(n)} \tag{1}$$

where $\underline{u}(t)$ denotes the time varying vector of displacements of all finite element degrees of freedom. Further, the vectors $\underline{\psi}^{(n)}$ are specified, constant basis functions and $q_n(t)$ are the corresponding time dependent generalized coordinates.

In this light, there are three key aspects in the development of nonlinear reduced order models:

(a) the selection of the basis functions $\underline{\psi}^{(n)}$,

(b) the derivation of the governing (differential) equations for the generalized coordinates $q_n(t)$.

In fact, these governing equations will be found to be parametric, i.e. their *form* is the same (generalized Duffing equations) for all structures and all basis functions but the *parameters* they involve will depend on both structure

and basis functions, exactly as the stiffness matrix in linear systems. Thus, the third key aspect is:
(c) the determination of the parameters of the governing equations of (b).

Note that steps (a) and (c) will be achieved non-intrusively from a commercial finite element model.

These three aspects of the nonlinear reduced order modeling technique will be briefly reviewed in the next sections.

A. Selection of the Basis

The appropriate selection of the basis functions $\underline{\psi}^{(n)}$ is critical for the accuracy of the reduced order model predictions. If the response of the full finite element model is not well represented within the basis, a poor prediction generally results. Yet, constructing a reliable basis is notably more difficult than it is for a linear structure where the basis is composed of the modes in the frequency band of the excitation which exhibit a sufficiently large modal force.

Clearly, the basis functions required to model a nonlinear geometric response do include those used for the corresponding linear problem, but others are also needed to capture the difference in physical behavior induced by the nonlinearity. This situation is particularly clear in shell-like structures subjected to transverse loadings in which the linear response is predominantly transverse while the tangential/in-plane displacement field provides the important "membrane-stretching" effect (see [2,6,7] for discussion).

This issue was addressed in [5] through an additional set of basis functions referred to as dual modes aimed at capturing the membrane stretching effects. The key idea in this approach is to first subject the structure to a series of "representative" static loadings, and determine the corresponding *nonlinear* displacement fields. Then, extract from them additional basis functions, the "dual modes". More specifically, it was argued in [5] that the representative static loadings should be selected to excite primarily the linear basis modes and, in fact, in the absence of geometric nonlinearity (i.e. for a linear analysis) should only excite these modes.

The specific details of the construction of the dual modes from the finite element model can be found in [2,3,5]. Once found, they will be appended to the modes that would be used in the linear case to form the basis for the representation of the nonlinear response.

B. Governing Equations for the Genralized Coordinates

A detailed derivation of the governing equations for the generalized coordinates $q_n(t)$ is presented in [2,5]. A brief review is presented here to support the inconsistency discussion, item (i) of section I. The desired governing equations are derived from the equations of finite deformation elasticity in the undeformed configuration Ω_0.

Specifically, the equations of motion for an infinitesimal element are (summation is implied over repeated indices)

$$\frac{\partial}{\partial X_k}\left(F_{ij}\, S_{jk}\right) + \rho_0\, b_i^0 = \rho_0\, \ddot{u}_i \tag{2}$$

where $\underline{\underline{S}}$ is the second Piola-Kirchhoff stress tensor, ρ_0 denotes the density in the reference configuration, and $\underline{b}^0$ is the vector of body forces, all of which are assumed to depend on the position $\underline{X} \in \Omega_0$. In Eq. (2), $\underline{\underline{F}}$ denotes the deformation gradient tensor of components

$$F_{ij} = \frac{\partial x_i}{\partial X_j} = \delta_{ij} + \frac{\partial u_i}{\partial X_j} \tag{3}$$

where δ_{ij} is the Kronecker delta and $\underline{u} = \underline{x} - \underline{X}$ is the displacement vector, $\underline{x}$ being the position vector in the deformed configuration. The material is assumed here to be linear elastic in that $\underline{\underline{S}}$ and $\underline{\underline{E}}$ (the Green strain tensor) satisfy

$$S_{ij} = C_{ijkl}\, E_{kl} \tag{4}$$

where $\underline{\underline{C}}$ is a fourth order elasticity tensor, function in general of the undeformed coordinates $\underline{X}$.

In parallel to its discrete counterpart in Eq. (1), the displacement field u_i in the continuous structure is sought in the modal-like representation

$$u_i(\underline{X}, t) = \sum_{n=1}^{M} q_n(t)\, U_i^{(n)}(\underline{X}) \qquad i = 1,2,3 \tag{5}$$

where $U_i^{(n)}(\underline{X})$ are specified, constant basis functions satisfying the boundary conditions also in the undeformed configuration.

A set of nonlinear ordinary differential equations governing the evolution of the generalized coordinates $q_n(t)$ can then be obtained by introducing Eq. (5) in Eqs (2)-(4) and imposing (Galerkin approach) the error to be orthogonal to the basis. This process leads [5] to the requisite reduced order model equations

$$M_{ij}\ddot{q}_j + D_{ij}\dot{q}_j + K_{ij}^{(1)} q_j + K_{ijl}^{(2)} q_j q_l + K_{ijlp}^{(3)} q_j q_l q_p = F_i \quad . \tag{6}$$

Note in Eq. (6) that a linear damping term $D_{ij}\,\dot{q}_j$ has been added to collectively represent various dissipation mechanisms. Further, M_{ij} denotes the elements of the mass matrix, $K_{ij}^{(1)}$, $K_{ijl}^{(2)}$, $K_{ijlp}^{(3)}$ are the linear, quadratic, and cubic stiffness coefficients and F_i are the modal forces.

Equations (6) are the desired governing equations. Note that their form (cubic nonlinearity on stiffness, or generalized Duffing) is the same irrespectively of the structure considered or the basis adopted to represent its motion. What does depend on the structure and the basis are the stiffness coefficients and their identification from the finite element model represents the last key step below.

C. Identification of the Stiffness Coefficients

The identification of the linear, quadratic, and cubic stiffness coefficients from a finite element model given a basis has been reviewed in details in [2] with a novel approach based on the availability of the tangent stiffness matrix described and validated in [3]. These strategies can broadly be divided into those in which the responses to a prescribed set of loads is used and those which rely on imposed sets of displacements and the forces that are required to accomplish them. The latter approach is followed here.

To exemplify its applications, assume first that a static displacement field (no summation over *n*)

$$\underline{u} = q_n\ \underline{\psi}^{(n)} \tag{7}$$

is imposed on the structure. Introducing this equality in Eq. (6) leads to the relation

$$K_{in}^{(1)} q_n + K_{inn}^{(2)} q_n^2 + K_{innn}^{(3)}\ q_n^3 = F_i \quad \text{(no sum on } n\text{)} \tag{8}$$

where F_i denotes the modal forces obtained by projecting the finite element forces necessary to induce the displacement of Eq. (7) on the basis $\underline{\psi}^{(i)}$.

Imposing similar displacement fields but of different magnitudes, i.e.

$$\underline{\hat{u}} = \hat{q}_n\ \underline{\psi}^{(n)} \qquad \text{and} \qquad \underline{\tilde{u}} = \tilde{q}_n\ \underline{\psi}^{(n)} \tag{9}$$

leads to the equations

$$K_{in}^{(1)}\ \hat{q}_n + K_{inn}^{(2)} \hat{q}_n^2 + K_{innn}^{(3)}\ \hat{q}_n^3 = \hat{F}_i \quad \text{(no sum on } n\text{)} \tag{10}$$

and

$$K_{in}^{(1)}\ \tilde{q}_n + K_{inn}^{(2)} \tilde{q}_n^2 + K_{innn}^{(3)}\ \tilde{q}_n^3 = \tilde{F}_i \quad \text{(no sum on } n\text{).} \tag{11}$$

In fact, Eqs (8), (10), and (11) form a system of equations for the coefficients $K_{in}^{(1)}$, $K_{inn}^{(2)}$, and $K_{innn}^{(3)}$ for all *i*. Repeating this effort for $n = 1, ..., M$ thus yields a first set of stiffness coefficients.

Proceeding similarly but with combinations of two basis functions, i.e.

$$\underline{u} = q_n\ \underline{\psi}^{(n)} + q_m\ \underline{\psi}^{(m)} \quad m > n \tag{12}$$

and relying on the availability of the coefficients $K_{in}^{(1)}$, $K_{inn}^{(2)}$, $K_{innn}^{(3)}$ and $K_{im}^{(1)}$, $K_{imm}^{(2)}$, $K_{immm}^{(3)}$ determined above, leads to equations involving the three coefficients $K_{inm}^{(2)}$, $K_{innm}^{(3)}$, and $K_{inmm}^{(3)}$. Thus, imposing three sets of displacements of the form of Eq. (12) provides the equations needed to also identify $K_{inm}^{(2)}$, $K_{innm}^{(3)}$, and $K_{inmm}^{(3)}$.

Finally, imposing displacement fields as linear combinations of three modes, i.e.

$$\underline{u} = q_n\ \underline{\psi}^{(n)} + q_m\ \underline{\psi}^{(m)} + q_r\ \underline{\psi}^{(r)} \quad r > m > n \tag{13}$$

permits the identification of the last coefficients, i.e. $K^{(3)}_{inmr}$.

III. Flat Cantilever Beam

A. Background and Properties

The symmetry of any flat isotropic structure in the transverse direction implies a series of properties. First, the modes of the linear structure decouple into purely transverse and purely inplane modes, with the former retained in the reduced order model. Further, the dual modes as described in [2,3,5] will exhibit only inplane motions. Then, relying again on the symmetry of the structure and the above properties of the modes, it can be shown that all coefficients of the type $K^{(1)}_{td}$, $K^{(1)}_{dt}$, $K^{(2)}_{ttt}$, $K^{(2)}_{tdd}$, $K^{(2)}_{dtd}$, $K^{(3)}_{tddd}$, $K^{(3)}_{dtdd}$, $K^{(3)}_{tttd}$, and $K^{(3)}_{dttt}$ must vanish for any transverse mode *t* or combination thereof and any dual mode *d* or combination thereof. The governing equations for a one transverse (mode 1) one dual (mode 2) reduced order model (1T1D model) are thus

$$M_{11}\ddot{q}_1 + C_{11}\dot{q}_1 + K^{(1)}_{11}q_1 + K^{(2)}_{112}q_1q_2 + K^{(3)}_{1122}q_1q_2^2 + K^{(3)}_{1111}q_1^3 = F_1 \tag{14}$$

$$M_{22}\ddot{q}_2 + C_{22}\dot{q}_2 + K^{(1)}_{22}q_2 + K^{(2)}_{211}q_1^2 + K^{(2)}_{222}q_2^2 + K^{(3)}_{2112}q_1^2q_2 + K^{(3)}_{2222}q_2^3 = F_2\,. \tag{15}$$

Equations (14) and (15) are an *exact* 2-mode representation of the motions. These equations are often approximated by neglecting the nonlinear terms of the inplane generalized coordinate q_2 based either on (i) the use of the von Karman strain equations or (ii) on their expected "small" effect on the response as the inplane motions are "small". This assumption leads to the *approximate* model (referred to as "cleaned" model in the sequel)

$$M_{11}\ddot{q}_1 + C_{11}\dot{q}_1 + K^{(1)}_{11}q_1 + K^{(2)}_{112}q_1q_2 + K^{(3)}_{1111}q_1^3 = F_1 \tag{16}$$

$$M_{22}\ddot{q}_2 + C_{22}\dot{q}_2 + K^{(1)}_{22}q_2 + K^{(2)}_{211}q_1^2 = F_2 \quad . \tag{17}$$

For loadings that are either static or dynamic but with low excitation frequency, the dynamic terms of the inplane generalized coordinate are often neglected (this is exact for static problems, approximate for dynamic ones) resulting in the simplified version of Eq. (17)

$$K^{(1)}_{22}q_2 + K^{(2)}_{211}q_1^2 = F_2\,. \tag{18}$$

This equation can be solved for q_2 which can then be reintroduced in Eq. (16) to yield

$$M_{11}\ddot{q}_1 + C_{11}\dot{q}_1 + \left[K^{(1)}_{11} + \frac{K^{(2)}_{112}}{K^{(1)}_{22}}F_2\right]q_1 + \left[K^{(3)}_{1111} - \frac{K^{(2)}_{112}K^{(2)}_{211}}{K^{(1)}_{22}}\right]q_1^3 = F_1\,. \tag{19}$$

The two terms in brackets in the above equation represent the equivalent linear and cubic stiffnesses of the transverse motions. No quadratic term is present owing to the symmetry of the structure. The cubic stiffness term was of particular interest in [4] where it was shown that its value

$$\hat{K}^{(3)}_{1111} = K^{(3)}_{1111} - \frac{K^{(2)}_{112}K^{(2)}_{211}}{K^{(1)}_{22}} \tag{20}$$

is much less, by four to five orders of magnitude in fact, than the "uncondensed" value $K^{(3)}_{1111}$. This observation indicates that the accuracy with which $\hat{K}^{(3)}_{1111}$ will be estimated is much less than that of the parameters it involves, e.g. $K^{(3)}_{1111}$. Yet, $\hat{K}^{(3)}_{1111}$ must be accurately identified as it is the only nonlinear term in Eq. (19) and stability requires a stiffening behavior, i.e. $\hat{K}^{(3)}_{1111} \geq 0$.

This identification challenge was resolved in [4] by estimating and combining two different models. The first is a cleaned model of the form of Eqs (16) and (17) involving both transverse and inplane motions. The second is a condensed model as in Eq. (19) which led to a positive identified value of $\hat{K}^{(3)}_{1111}$ from which the parameter $K^{(3)}_{1111}$ was then determined using Eq. (20). This methodology was delineated in [4] for reduced order models involving arbitrary numbers of transverse and dual modes and was validated on a series of flat beams and plate structures, an excellent matching of full finite element results being obtained.

Since the procedure of [4] relies extensively on Eqs (16) and (17), it is technically not applicable to curved structures for which Eqs (14) and (15), and thus Eqs (16) and (17), are not valid owing to non vanishing parameters $K_{td}^{(1)}$, $K_{dt}^{(1)}$, $K_{ttt}^{(2)}$, $K_{tdd}^{(2)}$, etc. Further, the separation of the modes into "transverse" and "inplane" is also unclear.

The initial focus of the revisit of the cantilever beam studied in [4], see Table 1 for dimensions and properties, was thus the search for an estimation procedure of the reduced order model parameters that would lead to a stable model, yet would not be dependent upon the symmetry properties assumed above.

Table 1. Flat Cantilevered Beam Properties

Beam Length	0.2286 m
Cross-section Width	0.0127 m
Cross-section Thickness	7.75 10-4 m
Mass per unit length	7875 kg/m3
Young's Modulus	205,000 MPa
Shear Modulus	80,000 MPa

B. Reduced Order Models and Their Stability

Proceeding in increasing order of complexity, a 2-mode (1T1D) model was first considered that is constructed with the first bending mode (transverse motion) of the beam and its associated dual. The stiffness parameters of this model were determined using the imposed displacements approach of section II.C but this first model was found to be unstable.

Next, the value of $\hat{K}_{1111}^{(3)}$ was computed from Eq. (20) to assess whether this stability problem resulted from an effective softening ($\hat{K}_{1111}^{(3)}$ <0) but this parameter was determined to be positive indicating a small but definite stiffening of the system. As a confirmation, the corresponding cleaned model of Eqs (16) and (17) was found to be stable. A similar effort was carried out with a 4-transverse 4-dual (4T4D) model exhibiting the same modes as in [4] and again the cleaned model was found to be stable. In fact, this model provided an excellent match of both transverse and inplane deflections computed by Nastran for the beam subjected to a single transverse tip force, see Fig. 3.

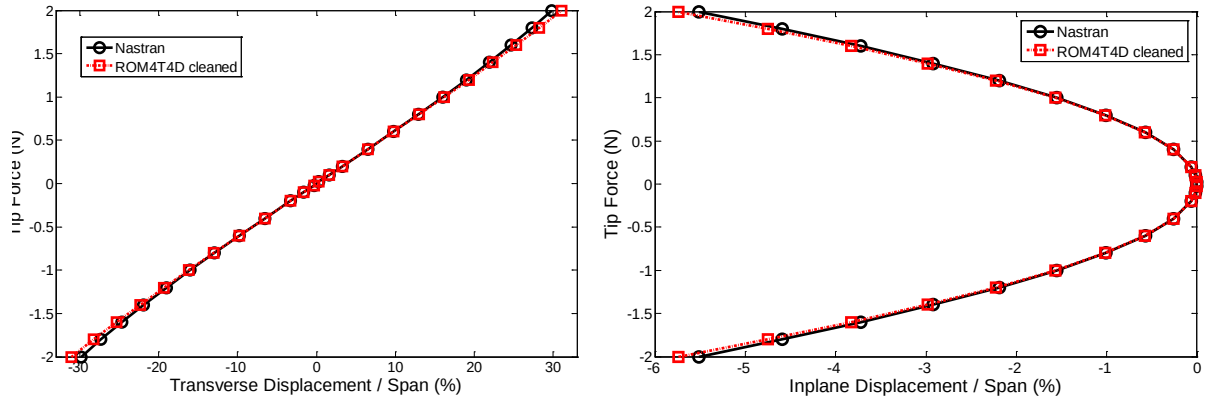

Figure 3. Comparison of Nastran and the cleaned 4T4D reduced order model. (a) transverse displacement; (b) inplane displacement. Cantilever beam with tip force.

These findings indicate that the instability originates from a different mechanism and two sources were considered, i.e. from

(i) the "small" nonlinear terms in the generalized coordinate q_2 that are present in Eqs (14) and (15) but were neglected in Eqs (16) and (17), and/or

(ii) the terms that should be zero due to symmetry but were identified to be small but nonzero.

To assess option (1), the response of the model of Eqs (14) and (15) was sought with the identified parameter values and instability of this model was indeed observed for transverse displacements of the order of 4% of the span (corresponding to more than 10 thicknesses). This finding was rather puzzling as the terms present in these equations but neglected when obtaining Eqs (16) and (17) seemed much smaller than those kept.

One possibility was that these terms were not identified properly thus leading to a fictitious instability problem. In this context, there are symmetry relations existing between model parameters, see [2,5], that arise from the existence of a potential energy associated with the structural deformations. These symmetry relations indicate that one should have $K^{(3)}_{1122} = K^{(3)}_{2112}$. These values were found to be $-2.17E+13$ and $-2.13E+13$ which are close enough to each other (2% difference) to suggest that these identified values were accurate. In fact, the identification was repeated under a series of different conditions and the values of $K^{(3)}_{1122}$ and $K^{(3)}_{2112}$ were consistently found around -2.1E+13. No symmetry condition exists for either $K^{(2)}_{222}$ or $K^{(3)}_{2222}$ which could not thus be validated in this manner, see section C below for a separate validation.

To better understand the occurrence of the instability, the four small terms were reintroduced in turn starting with the largest ones in magnitude, i.e. those associated with $K^{(3)}_{1122}$ and $K^{(3)}_{2112}$ leading to the model

$$M_{11}\ddot{q}_1 + C_{11}\dot{q}_1 + K^{(1)}_{11} q_1 + K^{(2)}_{112} q_1 q_2 + K^{(3)}_{1122} q_1 q_2^2 + K^{(3)}_{1111} q_1^3 = F_1 \tag{21}$$

$$M_{22}\ddot{q}_2 + C_{22}\dot{q}_2 + K^{(1)}_{22} q_2 + K^{(2)}_{211} q_1^2 + K^{(3)}_{2112} q_1^2 q_2 = F_2 . \tag{22}$$

Then, the relation between transverse excitation and transverse response was determined to clarify the nature of the instability. This analysis was carried out under static conditions and without inplane force, i.e. with $F_2 = 0$. Then, Eq. (22) can be used to solve for q_2 in closed form as

$$q_2 = -\frac{K^{(2)}_{211} q_1^2}{K^{(1)}_{22} + K^{(3)}_{2112} q_1^2} . \tag{23}$$

Reintroducing this expression in Eq. (21) leads to the desired relation between q_1 and F_1 in the form

$$K^{(1)}_{11} q_1 - \frac{K^{(2)}_{112}\, K^{(2)}_{211} q_1^3}{K^{(1)}_{22} + K^{(3)}_{2112} q_1^2} + \frac{K^{(3)}_{1122}\left[K^{(2)}_{211}\right]^2 q_1^5}{\left[K^{(1)}_{22} + K^{(3)}_{2112} q_1^2\right]^2} + K^{(3)}_{1111} q_1^3 = F_1 . \tag{24}$$

This complex relation is displayed graphically in Fig. 4 for a variety of values of $K^{(3)}_{1122} = K^{(3)}_{2112}$ for the flat beam under consideration. Note that the curve $F_1 = F_1(q_1)$ exhibits a maximum for negative values of $K^{(3)}_{1122} = K^{(3)}_{2112}$, indicating that no static solution exists for the transverse force exceeding this maximum. These observations were not affected by the other two small terms, the exact model of Eqs (14) and (15) exhibiting the same feature. Yet, such a solution is predicted by the full finite element model (Nastran here)!

A different perspective on the above issues can be obtained by analyzing the tangent stiffness matrix, K_T, which can be extracted in Nastran through a DMAP alter but can also be computed for the reduced order model. If the lowest eigenvalue of this matrix is positive, the system is stable.

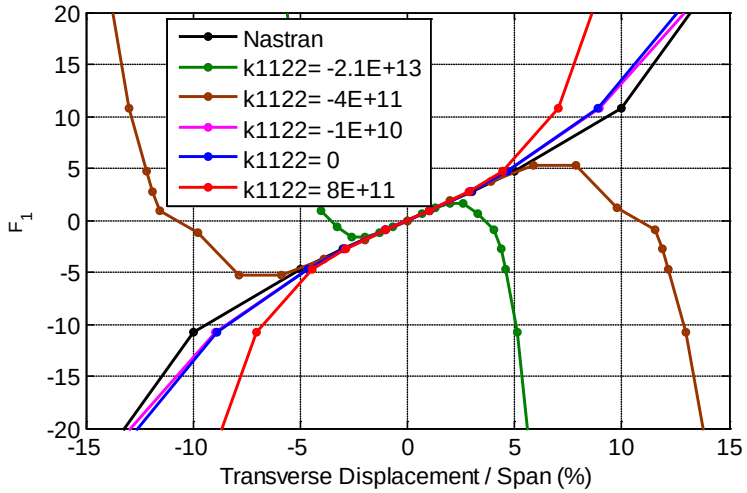

Figure 4. Transverse force vs. transverse displacement for the first mode of the cantilever beam, Nastran results and reduced order models with different $K^{(3)}_{1122}$ values.

Plotted in Fig. 5(a) as functions of the load are the first eigenvalues of the original 1T1D model, as compared with Nastran results generated by imposing transverse displacements proportional to the first (dominant) transverse mode at various levels. It can be seen that the eigenvalues of the 1T1D model are negative at most of the levels (actually it is positive only at the level of 1% of the span, where the model is stable), while the Nastran eigenvalues are positive. When the 1T1D model is cleaned, the first eigenvalues become positive as seen from Fig. 5(b). However, the curve of the cleaned 1T1D model does not match the Nastran curve.

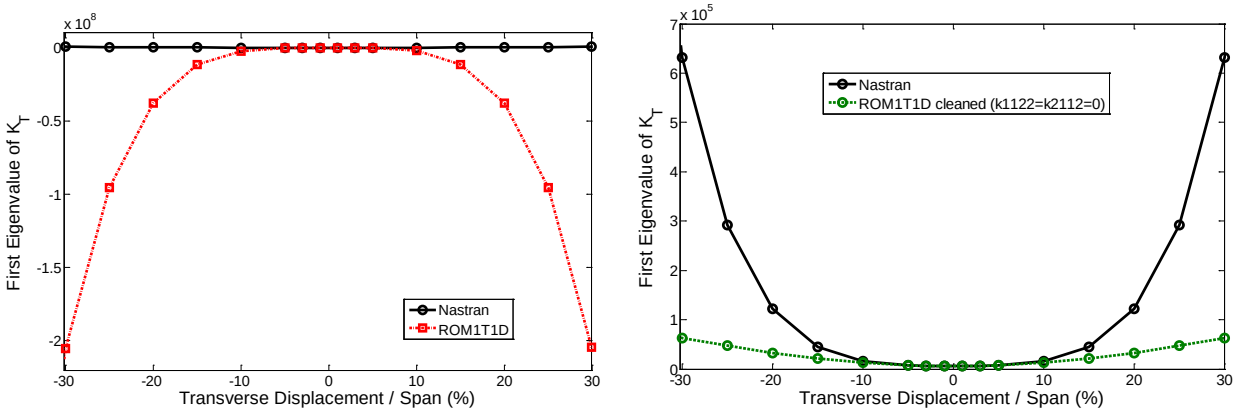

Figure 5. Comparison of first eigenvalues of tangent stiffness matrices from Nastran and the full 1T1D model. (a) the original 1T1D model; (b) the cleaned 1T1D model.

It was next desired to assess the effects of the parameter $K^{(3)}_{1122}$ (which is set equal to $K^{(3)}_{2112}$) on these eigenvalues. Then, shown in Fig. 6 are the curves of the first eigenvalue for various $K^{(3)}_{1122}$ values. Firstly, when keeping the $K^{(3)}_{1122}$ and $K^{(3)}_{2112}$ values as in the original 1T1D model, the eigenvalues (the solid red line) are positive up to the level of 15% of the span then become negative. If we set these parameters equal to -2.17E+13 (i.e. $K^{(3)}_{2112}$ changed from -2.13E+13 to -2.17E+13), the eigenvalues become negative at the level of 5% of the span. This result suggests a strong influence of $K^{(3)}_{1122}$ on the stability of the reduced order model. It also seems to suggest that the value of $K^{(3)}_{1122}$ should be either small if negative or positive. This condition is confirmed by the other curves of Fig. 6.

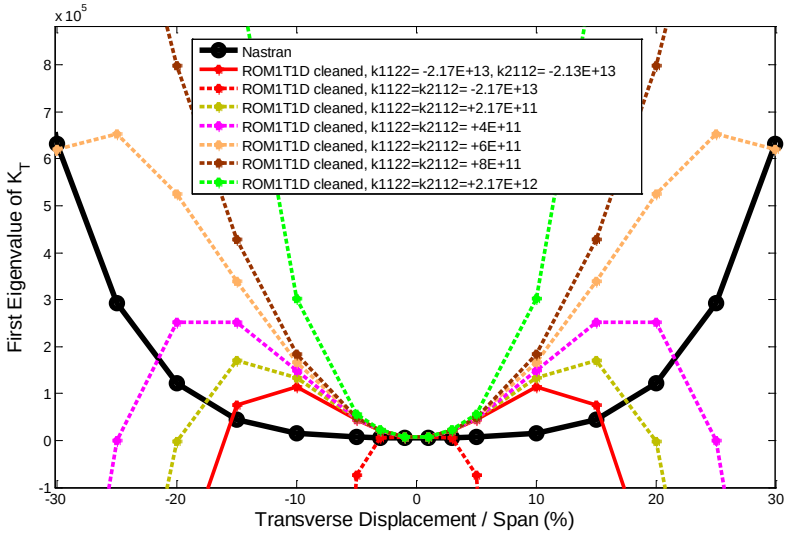

Figure 6. Influence of the parameter $K^{(3)}_{1122}$ on the first eigenvalue of the tangent stiffness matrices of the 1T1D reduced order model, cantilever beam.

Meanwhile, it can be seen that varying $K^{(3)}_{1122}$ alone cannot yield a close matching of the eigenvalue curves corresponding to Nastran and the reduced order model. So, the model may be stable but the predictions are not close to Nastran suggesting also that another coefficient may need to be adjusted. The first candidate would be $K^{(3)}_{1111}$, the cubic stiffness coefficient of the transverse mode, which plays a critical role in the response level of the model [4].

Accordingly, the value of $K^{(3)}_{1111}$ was varied with fixed values of $K^{(3)}_{1122}$ and $K^{(3)}_{2112}$ and the first eigenvalue of the tangent stiffness matrix was computed and monitored. It appears from Fig. 6 that the curve corresponding to $K^{(3)}_{1122}$ = 8E+11 is the one most similar to its Nastran counterpart and thus this value of $K^{(3)}_{1122}$ was adopted while varying $K^{(3)}_{1111}$. The results of varying this parameter are shown in Fig. 7. Note that the original value of $K^{(3)}_{1111}$ is 7.64E+12. It can be seen from Fig. 7 that when $K^{(3)}_{1111}$ is set to be 7.613E+12, the curve of the 1T1D model matches the Nastran curve quite well up to the level of 25% of the span. The closeness of this value of $K^{(3)}_{1111}$ to its originally identified one suggests that the cubic terms involving the dominant transverse motions are accurately estimated, although possibly not as well as required for $\hat{K}^{(3)}_{1111}$.

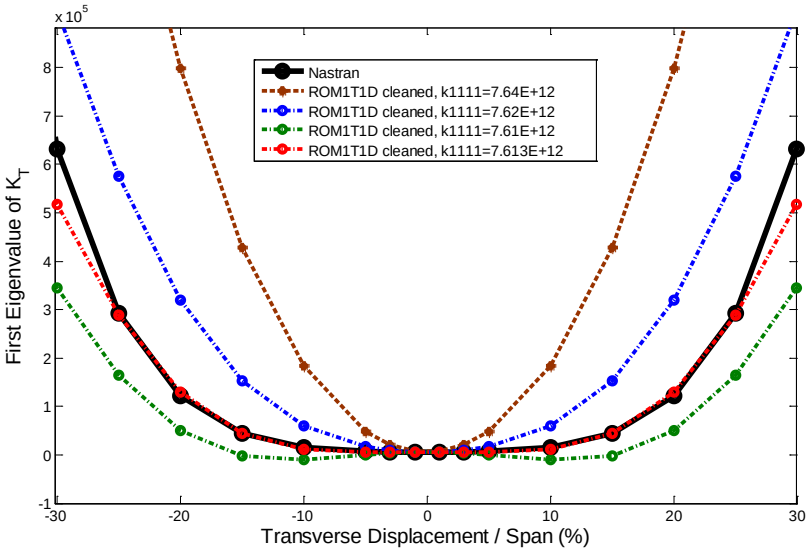

Figure 7. Influence of the parameter $K^{(3)}_{1111}$ on the first eigenvalue of the tangent stiffness matrices of the 1T1D reduced order model with $K^{(3)}_{1122}$ = $K^{(3)}_{2112}$ = 8E+11, cantilever beam.

C. Flat Cantilever Beam: Summary of Findings

The above findings indicate that the reduced order model identified under small deformations is not applicable to the large deformations observed in cantilever structures. It is believed that this issue arises from the difference in definition of linear elasticity which is in the deformed configuration for Nastran while it is in the undeformed one for the reduced order modeling. That is, the inconsistency pointed in (i) in section I.

The above discussion further indicates that some of the parameters are correctly obtained and these would include the quadratic terms (as they relate to the buckling limit for example which is correctly estimated) and the cubic terms of the transverse motions with the potential limitations of the identification approach described above and in [4].

To provide a formal confirmation of the above expectations, the reduced order modeling approach devised in [8] in a full Lagrangian framework was applied to a block element model of the above cantilevered beam. This effort led to the coefficients of a 1T1D model shown in Table 2 and that model was found to be stable. Also shown in this table are the coefficients as identified from Nastran per the procedure of section II.C with the same linear and dual modes. The matching of the quadratic term ($K^{(2)}_{112}$) and the leading cubic term ($K^{(3)}_{1111}$) between these two

formulations is excellent as expected. Note however the large discrepancy between the coefficients $K^{(3)}_{1122}$ obtained with the two approaches. Further, the value of that coefficient for the Lagrangian approach of [8] is positive as is required for stability per the discussion of section B above vs. negative (and thus unstable) for the model identified as in section II.C. The matching of the coefficients $K^{(2)}_{222}$ or $K^{(3)}_{2222}$ is also poor.

Table 2. Comparison of the Coefficients Identified by the Full Lagrangian Approach and the Nastran Procedure.

	Full Lagrangian [8]	Nastran Procedure (Section II.C)
$K^{(2)}_{112}$	3.8927E+11	3.8922E+11
$K^{(3)}_{1111}$	2.7552E+13	2.7547E+13
$K^{(3)}_{1122}$	2.8146E+13	-3.6627E+13
$K^{(2)}_{222}$	5.9545E+11	4.7266E+06
$K^{(3)}_{2222}$	2.0612E+13	-2.6951E+08

This comparison suggests that the cleaning procedure discussed above appropriately focuses on terms that are affected by differences in finite elememt formulations. In this light, the cleaning procedure is considered acceptable, especially when the "uncleaned" model is found to be unstable or gives unreliable predictions.

IV. Curved Cantilever Beam

The next structure considered in this effort is a curved cantilever beam to assess the validity/relevance of the above findings in the more general setting of a non-flat structure. The curved beam studied in [9] was used in this analysis, except that the boundary conditions were changed from clamped-clamped to clamped-free (cantilever). The beam has an elastic modulus of 10.6E+6 psi, shear modulus of 4.0E+6 psi, and density of 2.588E-4 lbf-sec^2/in^4. The span of the beam is 18 inches, and its cross section is rectangular with thickness 0.09 inch and width 1 inch. The radius of curvature is 81.25 inch, and the rise of the curvature at the center of the beam is 0.5 inch.

For the curved beam, a reduced-order model of 2 linear modes and 2 dual modes (2L2D) was considered. As observed in connection with the flat cantilever beam, the original full model is unstable, but the cleaned model is stable and gives very good predictions as shown in Figs. 8(a) and 8(b), even though one expects that the parameters zeroed out in this process are not actually zero.

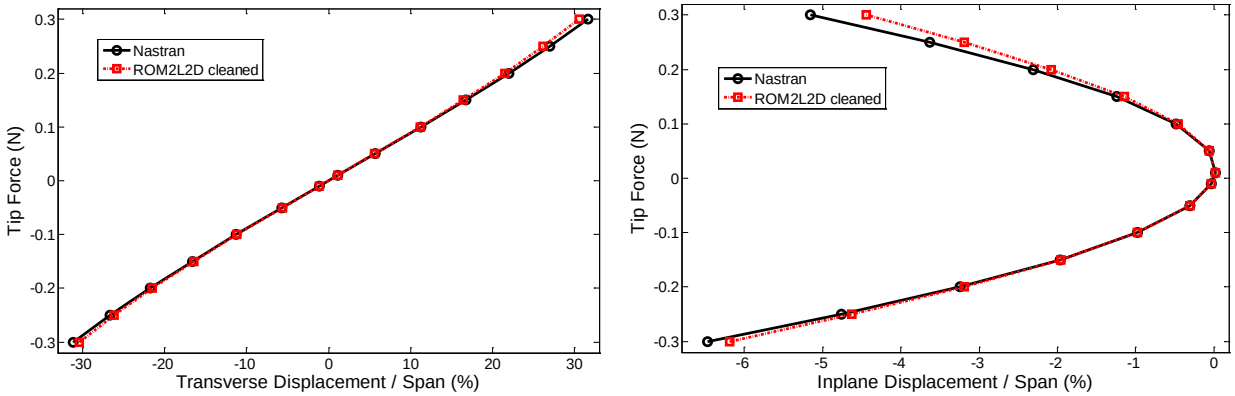

Figure 8. Comparison of predicted responses by Nastran and the cleaned full 2L2D reduced-order model. (a) transverse displacement; (b) inplane displacement, curved beam.

V. Predator Structural Modeling

A. Basis Selection

Consistently with the discussion of section II, the first step in the construction of a reduced order model for the Predator wing was the selection of the basis, starting with the linear modes. Their determination was achieved by

considering:
(1) the frequency band of the excitation in the planned aeroelastic application.
(2) the modes responding most to a set of "representative" loadings which were selected here as pressure distribution constant and or linear varying along span and chord.
These considerations led to the selection of the first 7 linear modes as key for the representation of the dominant motions.

As discussed in section II.A, it is necessary to enrich the linear basis when considering nonlinear geometric deflections because of the membrane stretching effect. The inclusion of purely linear modes, dominated by transverse deflections would lead to a model in which the end section of the wing would exhibit large transverse deflections with little shortening. This is not the behavior of the physical wing that exhibits a notable rotation so that the "effective" span reduces slightly but importantly as the transverse deflection increases. These spanwise dominated motions must be included in the model to correctly capture the wing's large displacement behavior and this represents the purpose of the dual modes of [5]. These modes are constructed (see [5]) as follows. First, the dominant linear modes retained are selected. In the present case, only a single dominant mode was considered, i.e. mode 1 which corresponds to the first wing bending mode. Next, a series of static loadings were applied to the wing that would induce only a response of the structure along the first mode if the structure was behaving linearly. The loading to be introduced is simply of the form

$$\underline{F} = \alpha \, K_{GG} \, \underline{\psi}_1 \tag{25}$$

where $\underline{F}$ is the vector of nodal forces, K_{GG} is the wing's finite element stiffness matrix, $\underline{\psi}_1$ is the first linear mode, and α is a coefficient varied to impose a particular deflection level.

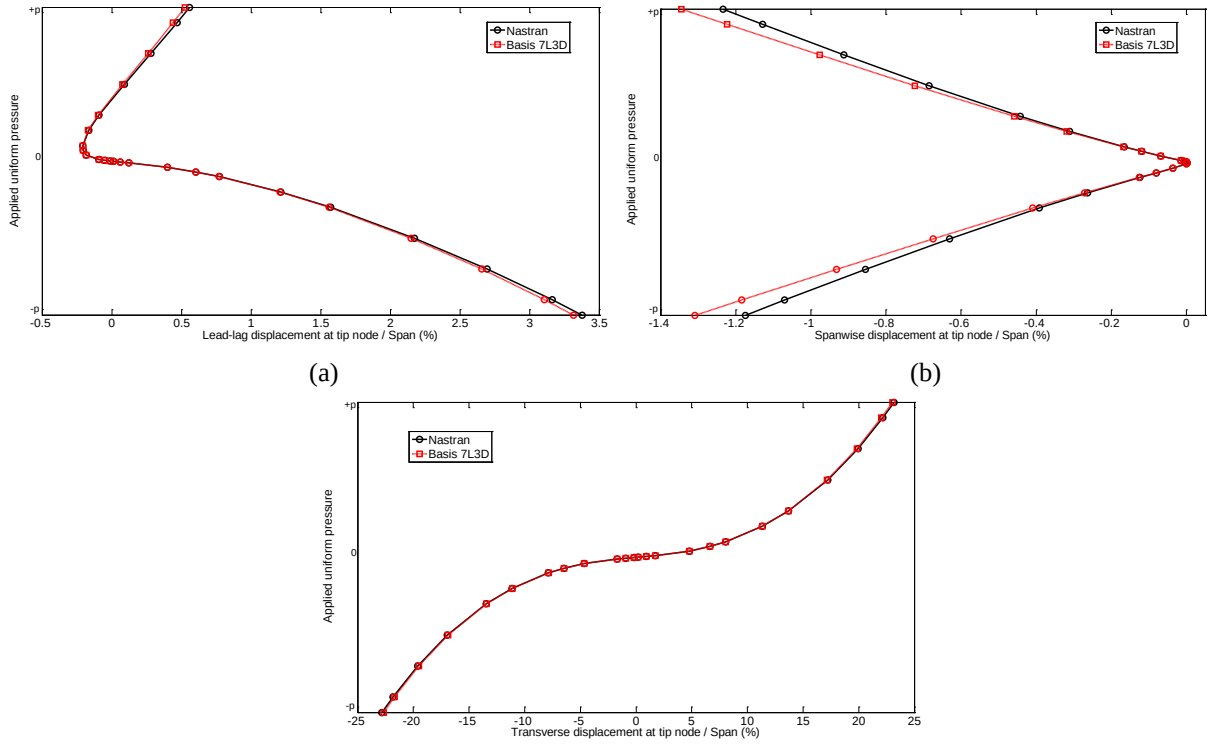

(a) (b)

(c)

Figure 9. Lead-lag (a), spanwise (b), and transverse (c) deflections of the tip leading edge of the Predator wing under a uniform load, Nastran and projection of Nastran results on the reduced order model basis.

An ensemble of 10 different loadings of this type were imposed on the predator wing leading to peak deflections ranging from -10 to +10 % of span. The processing of the 10 static displacement fields was achieved as in [5] by extracting first from these displacements their projections on the 7 modes forming the linear basis. A proper orthogonal decomposition (POD) analysis was then performed to obtain the dominant response features. Finally, a

potential energy based metric was evaluated to assess whether these modes would simply be slightly higher frequency transverse modes or truly high frequency components as desired.

The above dual construction was also repeated with loadings that would lead to responses, in the linear case, that are proportional to linear combinations of modes 1 and 2 and modes 1 and 3. This process ultimately led to the selection of 3 duals modes the displacements of which are spanwise dominated as expected.

The next step of the model construction is the verification of the appropriateness of the basis. This verification is achieved by projecting the responses obtained in a series of full nonlinear Nastran solutions (SOL 106) on the basis and comparing the Nastran displacement fields with their reconstruction from these projections. In terms of norm errors, it is found that the 10-mode model (referred to as 7L3D) gave low relative norm errors of 1%, 1%, and 0.1% in the lead-lag, spanwise, and transverse directions for a typical case, i.e. corresponding to a displacement equal to 8% of span. Another aspect of the model verification is the comparison of the deflections obtained from Nastran and from the projection on the basis. This aspect of the verification is performed graphically in Fig. 9 from which it is seen that the projection of the responses on the basis are indeed very close to their Nastran counterparts, suggesting the applicability of the basis.

B. Reduced Order Model Stability and Predictions

Next, the nonlinear stiffness coefficients of the 7L3D model were identified using the method described in section II.C, and its stability was checked. As observed in an earlier investigation [4], the stability limit of the model is limited to maximum deflections that are only a very small fraction of the span, e.g. of the order of 1%. The model is accordingly not readily usable as built. However, the detailed analysis of the flat cantilever beam and the brief study of the curved one suggest the following steps:

(i) zero out all cubic coefficients except those associated solely with the 7 linear modes

(ii) perform small modifications of these cubic coefficients, most notably the one associated with the largest response and possibly the quadratic ones, to improve the matching with Nastran data obtained in large deformations.

As already observed in connection with both flat and curved cantilevered beam, the reduced order model of the Predator wing after the cleaning process of step (i) was found to be stable up to 25% but leading to a significant underprediction of the Nastran response, see Figs 10-12 (model 7L3D -1).

As discussed in the flat beam section, a small change in the cubic coefficient of the dominant mode (mode 1) may be necessary because of the difficulty of getting an estimate of it accurate enough considering the softening of the inplane terms. Specifically, a change in $K_{1111}^{(3)}$ from 109 to 105 led to a very close matching of the Nastran results in the spanwise and transverse directions, see Figs 10 and 11, and an acceptable one in the lead-lag direction, see Fig. 12 (model 7L3D-2).

Further improvements of the lead-lag direction prediction was attempted by varying the parameters coupling the first and second lead-lag modes (modes 3 and 5 in the model) and the first bending mode (mode 1), i.e. $K_{5111}^{(3)}$ and $K_{311}^{(2)}$. This effort led to the model denoted as 7L3D-3 with improved matching shown as shown in Fig. 12.

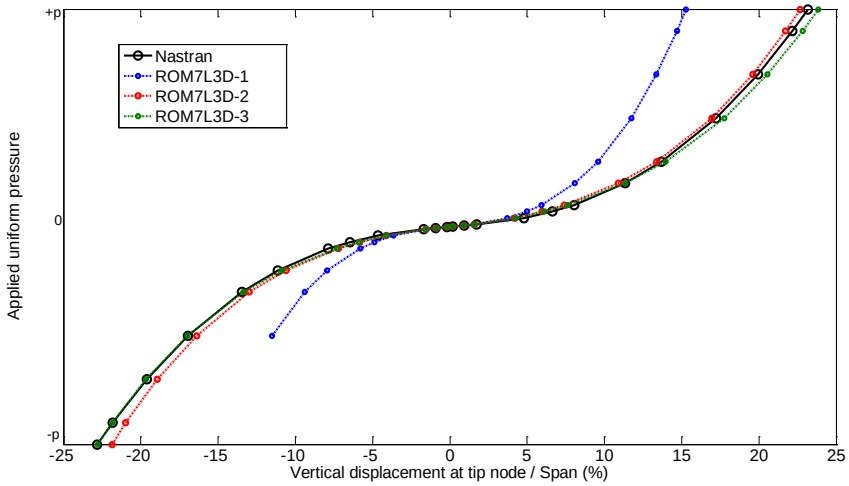

Figure 10. Vertical displacement of the Predator tip under uniform vertical force. Nastran results and predictions from the three reduced order models.

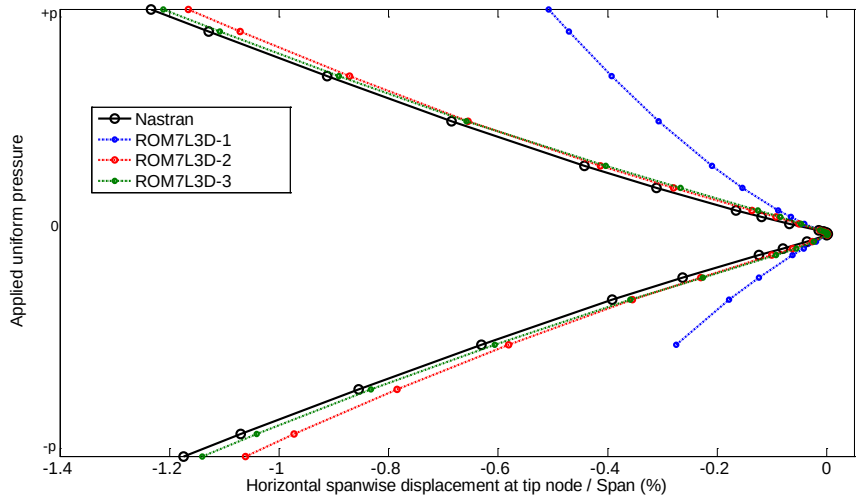

Figure 11. Horizontal spanwise displacement of the Predator tip under uniform vertical force. Nastran results and predictions from the three reduced order models.

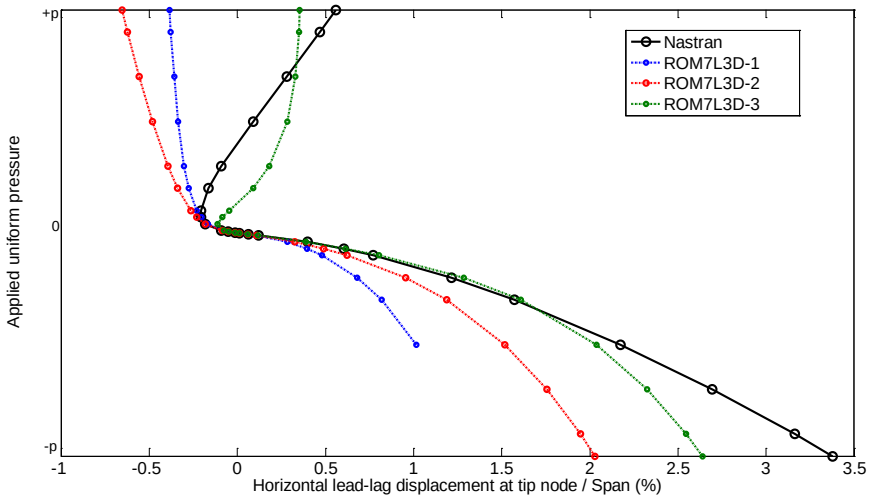

Figure 12. Horizontal lead-lag displacement of the Predator tip under uniform vertical force. Nastran results and predictions from the three reduced order models.

VI. Summary

The focus of this investigation was on a revisit of the construction of nonlinear reduced order models of cantilevered structures from finite element models developed in commercial software (Nastran here). This process involves most notably the selection of an appropriate basis and the identification of the parameters of the reduced order model from a series of finite element computations. Difficulties in carrying out the identification in connection with cantilevered structures had been reported in the past [4] where it had been suggested that differences in formulations of the finite element code and the reduced order model were responsible for the numerical instability shown by some identified models.

The above issues were revisited here, first in connection with a straight cantilevered beam of which a two-mode (1T1D) model was extensively considered. The identification approach of section II.C gave very consistent values of the model coefficients which further accurately satisfied necessary symmetry conditions. Yet, it was shown that one of these coefficients could simply not be correct as it forced the reduced order model to become numerically unstable at diplacements only fractions of the span. These observations clearly point to a difference in the formulations between finite element code and reduced order model. A formal confirmation of the above expectations was obtained by applying the reduced order modeling approach devised in [8] to the cantilevered beam model. This effort further confirmed which coefficients are most affected by the formulation differences. In this light, the palliative approach of [4] (the "cleaning" of coefficients) which consists in zeroing this last set of

coefficients may be considered acceptable, especially when the "uncleaned" model is found to be unstable or gives unreliable predictions.

This approach was confirmed on a curved cantilevered beam model and finally on a full finite element model of the Predator wing for which an excellent match between displacements predicted by the reduced order model and Nastran was observed. These results demonstrate the strong potential of reduced order models of nonlinear geometric structures, even those with very complex finite element models.

Acknowledgements

The financial support of this work by the contract NNX11CB68C from NASA Dryden Flight Research Center is gratefully acknowledged. In addition, we would like to thank Dr. Martin Brenner, the Technical Point of Contract, for his support of this contract.

References

[1] http://www.ga-asi.com/resources/library/index.php/Images/Aircraft-Platforms/Predator, extracted 09/05/2012.

[2] Mignolet, M.P., Przekop, A., Rizzi, S.A., and Spottswood, S.M., 2013, "A Review of Indirect/Non-Intrusive Reduced Order Modeling of Nonlinear Geometric Structures," *Journal of Sound and Vibration*, Vol. 332, No. 10, pp. 2437-2460.

[3] Perez, R., Wang, X.Q., and Mignolet, M.P., "Reduced Order Model for the Geometric Nonlinear Response of Complex Structures," *Proceedings of the 24th ASME Mechanical Vibration and Noise Conference*, Aug. 12-15, 2012, Chicago, Illinois, ASME Paper DETC2012/MECH-71141.

[4] Kim, K., Khanna, V., Wang, X.Q., and Mignolet, M.P., "Nonlinear Reduced Order Modeling of Flat Cantilevered Structures," *Proceedings of the 50th Structures, Structural Dynamics, and Materials Conference*, Palm Springs, California, May 4-7, 2009. AIAA Paper AIAA-2009-2492.

[5] Kim, K., Radu, A.G., Wang, X.Q., and Mignolet, M.P., 2013, "Nonlinear Reduced Order Modeling of Isotropic and Functionally Graded Plates," *International Journal of Non-Linear Mechanics*, Vol. 49, pp. 100-110.

[6] Hollkamp, J.J., Gordon, R.W., and Spottswood, S.M., "Nonlinear Modal Models for Sonic Fatigue Response Prediction: A Comparison of Methods," Journal of Sound and Vibration, Vol. 284, pp. 1145-1163, 2005.

[7] Hollkamp, J.J., and Gordon, R.W., 2008, "Reduced-Order Models for Nonlinear Response Prediction: Implicit Condensation and Expansion," *Journal of Sound and Vibration*, Vol. 318, pp. 1139–1153.

[8] Capiez-Lernout, E., Soize, C., and Mignolet, M.P., 2012, "Computational Stochastic Statics of an Uncertain Curved Structure with Geometrical Nonlinearity in Three-Dimensional Elasticity," *Computational Mechanics*, Vol. 49, No. 1, pp. 87-97.

[9] Chang, Y.-W., Wang, X.Q., Capiez-Lernout, E., Mignolet, M.P., and Soize, C., "Reduced Order Modeling for the Nonlinear Geometric Response of Some Curved Structures," *Proceedings of the 2011 International Forum of Aeroelasticity and Structural Dynamics*, Jun. 26-30, 2011, Paris, France, IFASD-2011-185.